Three-Phase Unbalanced Transient Dynamics and Powerflow for Modeling Distribution Systems With Synchronous Machines

Marcelo A. Elizondo, *Member, IEEE*, Francis K. Tuffner, *Member, IEEE*, and Kevin P. Schneider, *Senior Member, IEEE*

***Abstract*—Unlike transmission systems, distribution feeders in North America operate under unbalanced conditions at all times, and generally have a single strong voltage source. When a distribution feeder is connected to a strong substation source, the system is dynamically very stable, even for large transients. However if a distribution feeder, or part of the feeder, is separated from the substation and begins to operate as an islanded microgrid, transient dynamics become more of an issue. To assess the impact of transient dynamics at the distribution level, it is not appropriate to use traditional transmission solvers, which generally assume transposed lines and balanced loads. Full electromagnetic solvers capture a high level of detail, but it is difficult to model large systems because of the required detail. This paper proposes an electromechanical transient model of synchronous machines for distribution-level modeling and microgrids. This approach includes not only the machine model, but also its interface with an unbalanced network solver, and a powerflow method to solve unbalanced conditions without a strong reference bus. The presented method is validated against a full electromagnetic transient simulation.**

***Index Terms*—Distribution systems, machine models, microgrids, transient stability, unbalanced operation.**

NOMENCLATURE

$[I_{GSa,b,c}]$	Vector of machine Norton current sources in abc coordinates.
$[J]$	Jacobian matrix of powerflow current injection method.
$[T_s]$	Transformation matrix between abc and sequence coordinates.
$[Y_{\text{bus},abc}]$	System admittance matrix in abc coordinates.
$[Y_{Ga,b,c}]$	Matrix of machine subtransient admittances in abc coordinates.
$[\Delta I_{\text{bus},abc}]$	Vector of mismatch bus current injections for powerflow current injection method.
$[\Delta V_{\text{bus},abc}]$	Vector of incremental bus voltages for powerflow current injection method.
$[V_{Ga,b,c}]$	Vector of generator phase terminal voltages.
$[V_{\text{bus},abc}]$	Vector of machine terminal voltage in abc coordinates.
$I^{\text{calc}}_{\text{bus},abc}$	Calculated bus current injection at each iteration of powerflow current injection method.
$I_{GS0,1,2}$	Machine Norton current sources in symmetrical component coordinates.
$[I_{GENabc}]$	Vector of machine terminal currents in abc reference.
$[I_{GSa,b,c}]$	Vector of machine internal current source injection in abc coordinates.
P_T, Q_T	Total terminal active and reactive generated power.
$P^{sp}_{\text{load}}, Q^{sp}_{\text{load}}$	Specified load active and reactive power for powerflow current injection method.
$Y_{G0,1,2}$	Machine subtransient admittances in symmetrical components coordinates.
δ	Rotor angular position.
$[E''_{a,b,c}]$	Vector of internal machine subtransient voltages in abc coordinates.
ω	Rotor mechanical speed.
ω_s	Rated rotor mechanical speed.
$\psi_{1d,2q}$	Flux linkages of direct and quadrature axis dampers.
D	Machine damping.
$E'_{d,q}$	Transient voltages for direct and quadrature axis.
$E''_{d,q}$	Subtransient voltages for direct and quadrature axis.
E_{fd}	Field voltage.
H	Inertia constant.
$I_{0,1,2}$	Zero, positive, and negative sequence stator currents.
$I_{d,q}$	Currents for direct and quadrature axis.
$R_{0,1,2}$	Zero, positive, and negative sequence resistances.
R_a	Armature resistance.
$T'_{do,qo}$	Open circuit transient time constants for direct and quadrature axis.
$T''_{do,qo}$	Open circuit subtransient time constants for direct and quadrature axis.

Manuscript received March 25, 2014; revised August 09, 2014 and October 30, 2014; accepted December 24, 2014. Date of publication January 28, 2015; date of current version December 18, 2015. This work was supported by the Department of Energy, Office of Electricity Delivery and Energy Reliability. The Pacific Northwest National Laboratory is operated for the U.S. Department of Energy by Battelle Memorial Institute under Contract DE-AC05-76RL01830. Paper no. TPWRS-00411-2014.

The authors are with Pacific Northwest National Laboratory, Seattle, WA 98109 USA(e-mail: Marcelo.Elizondo@pnnl.gov; Francis.Tuffner@pnnl.gov; Kevin.Schneider@pnnl.gov).

Color versions of one or more of the figures in this paper are available online at http://ieeexplore.ieee.org.

Digital Object Identifier 10.1109/TPWRS.2015.2389712

T_{mech}	Mechanical torque.
$V_{d,q}$	Machine terminal voltages in dq coordinates.
$x'_{d,q}$	Transient reactances for direct and quadrature axis.
$x''_{d,q}$	Subtransient reactances for direct and quadrature axis.
x_0	Zero sequence reactance.
x_l	Leakage reactance.

I. Introduction

MICROGRIDS are most commonly deployed to provide high reliability power to critical or remote end-use loads [1]. This is motivated by a desire for improved power quality or backup generation to increase reliability [1]. Currently, the deployment of microgrids is limited due to the costs of design, construction, and operation. One way to reduce the cost of a microgrid is to perform detailed analysis in the design phase, which will ensure the proper design margins without the need to excessively oversize equipment. In particular, electromechanical transient analysis of microgrids, with adequate representation of unbalanced conditions, is necessary to analyze events such as large load increases, transitions between interconnected and islanded operation, and responses to faults.

Full unbalanced conditions, and machine dynamics, can be modeled using detailed electromagnetic transient simulations software [2]. However, examining the dynamics of a full size distribution feeder is not always practical with an electromagnetic transient simulation. Simplified electromagnetic analysis, in the form of harmonics analysis, can accommodate full feeders and unbalanced conditions, but is often not tailored toward the temporal nuances of distribution system load models [3]. These load models can require multiple states and operational envelopes [4]. Furthermore, multi-state load models and standard distribution equipment models, such as voltage regulators and shunt capacitors, often do not exist in electromagnetic simulators. The ability to import existing distribution planning models, utilizing existing load modeling capabilities, will reduce the cost, and increase the accuracy, associated with distribution level, and microgrid, transient analysis.

While there are dynamics of interest at the distribution level, when the system is islanded as a microgrid, the dynamics become a significant concern. Microgrids contain both generation sources and load sinks, but they often lack a strong central voltage source. Electromechanical transient modeling of microgrids has often used transmission-level approaches. However, transmission-level electromechanical transient modeling leverages a balanced three-phase assumption [5]–[8]. To study unbalanced faults at the transmission level, symmetric sequence components are often used [6]. However, for distribution-level and microgrid applications, these assumptions are not valid [9]. A lack of line transposition, single-phase lateral lines, and unbalanced loads render both the balanced assumption and the symmetrical component method insufficient to properly model the distribution or microgrid system properly [9].

The first step for unbalanced dynamic simulation at the distribution level is creating the machine model. A three-phase subtransient synchronous machine model that accounts for unbalanced loading was formulated in [10] and [11]. Unbalanced operation was captured using a simplified, fundamental frequency model in phasor representation [6], [10], [12], [13]. This simplification allows representing the three-phase machine in full symmetrical components, where the positive sequence represents the main electrical torque, and the negative sequence current produces a torque in opposition. The total electrical torque is constant, facilitating the solution and determination of equilibrium [11]. However, the variation of electrical torque due to unbalanced operation reported in [14] is ignored. Furthermore, the initialization of the fundamental frequency model in phasor representation is still unresolved [11].

The second step for unbalanced dynamic simulation at the distribution level is incorporating the unbalanced feeder model. Traditional, three-phase, unbalanced powerflow can be solved using methods such as the Newton-Raphson current injection method [15]. While this method accounts for the three-phase unbalanced effects and meshed network topologies, it does not directly incorporate the dynamics and constraints of a synchronous machine under unbalanced loads. The unbalanced powerflow solver must be properly interfaced with the unbalanced synchronous machine model.

Synchronous distributed generators impose constraints on the maximum possible network unbalance. The unbalanced currents and voltages in a synchronous generator are subject to the physical symmetry of the generator windings. Chen *et al.* [16] proposed a distributed generator model for powerflow solutions that accounts for the physical symmetry. The model consists of balanced three-phase internal voltages behind impedances. The model proposed in [16] requires two conditions: pre-specification of machine total active and reactive power, and a reference bus that connects to a larger power system [17]. These two conditions are not met in isolated microgrids.

Three-phase voltage magnitude and angle cannot be arbitrarily defined in a microgrid. This poses challenges in the powerflow solution because known three-phase voltage is assumed at the slack bus [15], [17]. The powerflow solution of a microgrid without a strong central voltage source needs to be solved and may vary with time. This is further complicated by the need to initialize both the network interface and machine dynamics of the electromechanical transient simulations.

This paper presents the models and approach to resolve the issues associated with modeling electromechanical transients and powerflow analysis of an unbalanced three-phase distribution feeder or microgrid with synchronous generators. The proposed model considers full network and load model details, typical of distribution system analysis. The proposed powerflow solution is adequate for unbalanced microgrids with no strong central voltage source. The proposed solution provides correct boundary conditions for the initialization of machine models and determining an equilibrium. Additionally, machine model assumptions necessary to capture appropriate system-level effects of the microgrid are proposed.

The approach described is implemented in the GridLAB-D™ software [18], and provides a basis for more system-level

evaluation of microgrid operations. This paper is organized as follows. Section II gives background formulation for synchronous machine models and the three-phase powerflow solution. Section III describes the main contribution of this paper: 1) proposed assumptions for machine models; 2) the interface between machine model and unbalanced network powerflow; and 3) the network powerflow solution for correct initialization and simulation, including the case where no strong reference bus is present. Section IV shows the validation results with an electromagnetic transient simulation, as well as a larger demonstration system. Finally, Section V concludes the paper and describes future work.

II. Background and Motivation

Transient analysis of a power system consists of studying the system response to disturbances using models that represent transient effects of system elements. The fundamental dynamic model for power system analysis is the electromagnetic transient model. The electromagnetic transients model considers not only machine transients, but also the faster transients in network components such as line and load inductances and capacitances. Transient electromechanical models consider transients mainly in machines, ignoring the faster transients in lines and load inductances and capacitances [19]–[21]. This simplification is acceptable for large systems where the phenomenon of interest is the electromechanical interaction between machines; this also has the advantage of computational efficiency. This simplification is also appropriate for the efficient analysis of distribution feeders or large microgrids which have a large number of elements for the detailed representation of distribution lines, cables, and end-use loads.

A. Synchronous Machine Model

The unbalanced operation of three-phase synchronous machines is modeled using a simplified fundamental frequency model in phasor representation according to [5], [10], [12], and [13]. This allows for a representation of the machine in full symmetrical components, where the positive sequence represents the main electrical torque, and the negative sequence current produces a torque in opposition. The total electrical torque is constant, facilitating the solution and determination of equilibrium. The variation of electrical torque due to unbalanced operation reported in [11] and [14] is ignored. Instead, the average behavior of the electrical torque is approximated with the formulation in this section and additional assumptions described in Section III-A.

The machine electrical dynamic equations are built on the standard $dq0$ axis implementation, as described in [5] and [6]. The equations begin with the relationship between the d-axis changes in the flux and the transient voltages, as described in [5]:

$$T'_{qo}\frac{dE'_d}{dt} = -E'_d + (x_q - x'_q)\left[I_q - \frac{(x'_q - x''_q)}{(x'_q - x_l)^2}\left[\psi_{2q} + (x'_q - x_l)I_q + E'_d\right]\right] \quad (1)$$

$$T''_{do}\frac{d\psi_{1d}}{dt} = -\psi_{1d} + E'_q - (x'_d - x_l)I_d. \quad (2)$$

The second axis of the model, the q-axis, is updated in a similar manner using (3) and (4):

$$T'_{do}\frac{dE'_q}{dt} = E_{fd} - E'_q - (x_d - x'_d)\left[I_d - \frac{(x'_d - x''_d)}{(x'_d - x_l)^2}\left[\psi_{1d} + (x'_d - x_l)I_d - E'_q\right]\right] \quad (3)$$

$$T''_{qo}\frac{d\psi_{2q}}{dt} = -\psi_{2q} - E'_d - (x'_q - x_l)I_q. \quad (4)$$

These d- and q-axis quantities form part of the series of differential equations that eventually lead to the subtransient voltages in the machine. Equations (5), (6), and (7) describe how the voltages relate to the flux values and current components of the machine [5]:

$$E''_d = -x''_q I_q - \frac{(x''_q - x_l)}{(x'_q - x_l)}E'_d + \frac{(x'_q - x''_q)}{(x'_q - x_l)}\psi_{2q} \quad (5)$$

$$E''_q = -x''_d I_d + \frac{(x''_d - x_l)}{(x'_d - x_l)}E'_q + \frac{(x'_d - x''_d)}{(x'_d - x_l)}\psi_{1d} \quad (6)$$

$$E''_0 = -x_0 I_0. \quad (7)$$

The machine mechanical portion of the dynamic equations is described by (8) and (9):

$$\frac{d\delta}{dt} = \omega - \omega_s \quad (8)$$

$$\frac{2H}{\omega_s}\frac{d\omega}{dt} = T_{\text{mech}} - (E''_q I_q - E''_d I_d) - (R_2 - R_s)I_2^2 - D(\omega - \omega_s). \quad (9)$$

The full electromagnetic transient equations of the stator voltages are given in (10), (11), and (12) [5]:

$$\frac{dE''_d}{dt} = \frac{\omega}{\omega_s}E''_q + R_a I_q + V_q \quad (10)$$

$$\frac{dE''_q}{dt} = \frac{\omega}{\omega_s}E''_d + R_a I_d + V_d \quad (11)$$

$$\frac{dE''_0}{dt} = R_0 I_0 + V_0. \quad (12)$$

The typical assumptions for transient electromechanical models neglect the stator dynamics of the machine. Specifically, derivatives of the left-hand side of (10), (11), and (12) are replaced by an algebraic Laplace representation for the fundamental frequency. The speed dependency of stator voltages are also usually neglected. Under such these assumptions, ω is set equal to ω_s in the first term of the right-hand side of (10), (11), and (12) [7]. For the proposed approach, these assumptions are further discussed in Section III-A.

B. Powerflow Solution of Three-Phase Unbalanced Distribution Network

The network and loads of the distribution system are represented in full abc coordinates. The abc formulation allows a complete representation of line and load unbalances. The network solution proposed in this paper (discussed in Section III-C) is an extension of the Current Injection Method (CIM) method

presented in [15]. A compact formulation of the CIM method can be stated as

$$[\Delta I_{\text{bus},abc}] = [J][\Delta V_{\text{bus},abc}] \tag{13}$$

where $[J]$ is the Jacobian matrix, which is equal to the system admittance matrix, $[Y_{\text{bus},abc}]$, except for the block-diagonal elements that have to be updated at each iteration for constant current load and constant power loads. $[\Delta I_{\text{bus},abc}]$ is calculated from specified power based on load models at each phase as

$$\Delta I_{\text{bus},abc} = \frac{P^{\text{sp}}_{\text{load}} + jQ^{\text{sp}}_{\text{load}}}{V_{\text{bus},abc}} - I^{\text{calc}}_{\text{bus},abc}. \tag{14}$$

Note that with known (14), (13) is solved for $[\Delta V_{\text{bus},abc}]$ by inverting $[J]$. This solution is performed iteratively until $[\Delta I_{\text{bus},abc}] <$ tolerance. For details on this formulation and the structure of the matrices, see [15].

While the method of [15] will solve unbalanced three-phase powerflow problems, it does not consider constraints in the unbalance imposed by synchronous generators. This limitation will be addressed in Sections III-B and III-C.

C. Symmetry Constraint for Current and Voltage Unbalance at a Synchronous Machine

Chen *et al.* [16] proposed a distributed generator model for powerflow solutions that accounts for the symmetrical construction of synchronous generators. The model utilizes balanced three-phase internal voltages (symmetry in generator windings) behind three-phase impedances that account for effect of unbalanced voltages. This symmetry constraint was applied to PQ generator buses in [16], but neglected slack and PV generator buses. The extension to these buses in a microgrid setting is discussed in Section III-C.

The generator admittance matrices, according to [16], are formed by converting the sequence components, shown in (15):

$$[Y_{Ga,b,c}] = [T_s]\begin{bmatrix} Y_{G0} & 0 & 0 \\ 0 & Y_{G1} & 0 \\ 0 & 0 & Y_{G2} \end{bmatrix}[T_s]^{-1} \tag{15}$$

where

$$[T_s] = \frac{1}{\sqrt{3}}\begin{bmatrix} 1 & 1 & 1 \\ 1 & e^{j4\pi/3} & e^{j2\pi/3} \\ 1 & e^{j2\pi/3} & e^{j4\pi/3} \end{bmatrix}. \tag{16}$$

Utilizing these values and the model proposed in [16], the current injection contributions to a powerflow algorithm are given by

$$I_{GS1} = \frac{P_T + jQ_T + [V_{Ga,b,c}]^H[Y_{Ga,b,c}][V_{Ga,b,c}]}{V^*_{Ga} + e^{j4\pi/3}V^*_{Gb} + e^{j2\pi/3}V^*_{Gc}} \tag{17}$$

$$[I_{GSa,b,c}] = \frac{1}{3}\begin{bmatrix} 1 \\ e^{j4\pi/3} \\ e^{j2\pi/3} \end{bmatrix} I_{GS1}. \tag{18}$$

Note that this value represents only positive sequence current values. Due to the generator physical symmetry constraints, there are no negative and zero sequence current sources [16], so those values are set to zero.

D. Synchronous Machine Controllers: Governor and Automatic Voltage Regulator

For the proper simulation and control of a synchronous machine, generator control models are also defined in the GridLAB-D dynamic simulations. A simple governor and exciter model are implemented for testing the electromechanical transient model. The governor is a Woodward diesel governor (DEGOV1) that modifies the mechanical torque of the synchronous machine proportionally to its mechanical speed deviation. The exciter model is a simplified exciter system (SEXS) that modifies the generator field voltage (and hence its reactive power) to control the generator's terminal voltage (average voltage magnitude of all phases). DEGOV1 and SEXS models are commonly used in power system industry-grade transient electromechanical programs such as GE PSLF and Siemens PSS/E. Block diagrams or equations of these controllers are omitted in this paper for brevity, and can be found in user manuals of these software packages [19], [20].

III. Electromechanical Simulation of Unbalanced Microgrids

To properly simulate an unbalanced system with synchronous machines, the models described in Section II must be combined and integrated into the unbalanced three-phase network solver system. Three key items that must be considered in this integration are: overall assumptions on the synchronous machine model, the interface between the overall network solver and the synchronous machine model, and the initial powerflow solution.

A. Synchronous Machine Electromechanical Assumptions

Modeling a synchronous machine under unbalanced powerflow operations creates unique conditions in electromagnetic simulations. This section discusses the assumptions, and implications, of the electromechanical machine model in this paper.

One of the main impacts of unbalanced operation is that the electrical torque is not constant and the machine speed is never in equilibrium [11], [14]. This effect is captured by electromagnetic simulations because it is related to the instantaneous values of phase currents. In contrast, the effect of unbalances in the electromechanical model of this paper is captured as an approximation of an average effect, by considering the negative sequence current component in the electrical torque equation, (9) [11], [14]. This electromechanical model obtains an equilibrium in the machine speed that also represents an approximate moving average of speed variations due to the microsecond-level variations in electrical torque, similar to transmission solvers [19]–[21].

Secondly, the electromechanical simulations use a phasor model of the network elements. This means that voltage transients in elements such as inductances and capacitances are ignored under the assumption that these transients are faster than the phenomenon of interest. This simplification inherently affects the treatment of stator voltages in that the stator dynamics are neglected; derivatives of the left-hand side of (10), (11), and (12) are replaced by algebraic Laplace approximations for the fundamental frequency.

Finally, different from the assumptions in traditional electromechanical models, the model of this paper considers the speed

dependency of stator voltages. That is, ω is not set equal to ω_s in the first term of the right-hand side of (10) and (11). This assumption also implies that the mechanical torque, instead of electrical power, is considered in (9). The mechanical torque is also the link between the governor and the machine, instead of the mechanical power value used in most electromechanical models for transmission simulations.

B. Network Solution and Machine Dynamic Model Interface

Interfacing with powerflow solver described in [15] requires adjustments to the electromechanical machine model. The synchronous machine dynamic models are linked to the network solution by using Norton current source equivalents with shunt generator impedances [8], [16]. The current sources are symmetric to represent the generator physical symmetry. The generator shunt impedances of the Norton equivalent circuit account for the effects of unbalanced terminal voltages. The current source of the Norton equivalent circuit is given by

$$[I_{GS1}] = \left[\frac{\omega}{\omega_s} E''_{d,q}\right][Y_{G1}]. \tag{19}$$

$E''_{d,q}$ represents the combination of (5) and (6), with the effect of speed variation $(\omega)/(\omega_s)$ as discussed in Section III-A, and Y_{G1} represents the positive sequence sub-transient admittance of the generator [6].

The current of (19) remains symmetric, reflecting the physical constraints of the device. This allows the symmetry constraints of the physical generator to be maintained and accurately reflected in the unbalanced powerflow solution. Values for I_{GS1} are updated through appropriate integration methods using the machine dynamic equations of Section II.

Note that to calculate the terminal current injections at generator nodes, a post processing is needed once the network solution is found. The generator current injections at the terminal can be calculated as

$$[I_{GENa,b,c}] = [I_{GSa,b,c}] - [Y_{Ga,b,c}][V_{\mathrm{bus},a,b,c}] \tag{20}$$

where $I_{GSa,b,c}$ is the current source injection in abc coordinates behind the machine sub-transient admittance $Y_{Ga,b,c}$. $I_{GSa,b,c}$ is calculated using (17). Note once again that $I_{GSa,b,c}$ is a positive-sequence, three-phase, balanced current source that represents the machine physical symmetry constraints.

As an additional deviation from standard distribution powerflow methods, the frequency dependence of network and load impedance elements is built in the powerflow formulation of [15]. That is, the phasor value of every reactive element is re-evaluated as a function of the current electrical frequency of the system. This adjustment helps integrate the electrical frequency variations the electromagnetic simulator provides, but with a simplified, electromechanical-based implementation.

To sum up, with respect to the powerflow formulation of [15], the following modifications are proposed in this paper:

- inductances and reactances in the system $[Y_{\mathrm{bus},abc}]$, and hence in $[J]$ of (13), are time-variant as a function of the system frequency;
- to include the synchronous machines, the sub-transient machine admittance matrix $[Y_{Ga,b,c}]$ is lumped into $[Y_{\mathrm{bus},abc}]$. In $[J]$ of (13), this affects only the block-diagonal elements, since the generator sub-transient admittance matrix represent elements connected in shunt at the generator buses;
- the generator's Norton equivalent current sources, $[I_{GSa,b,c}]$, are added to the specified bus current injections, affecting the elements of $[\Delta I_{\mathrm{bus},abc}]$ of (13). Therefore (14) can be rewritten as

$$\Delta I_{\mathrm{bus},abc} = \frac{P^{\mathrm{sp}}_{\mathrm{load}} + jQ^{sp}_{\mathrm{load}}}{V_{\mathrm{bus},abc}} + [I_{GSabc}] - [I^{\mathrm{calc}}_{\mathrm{bus},abc}]. \tag{21}$$

Note that $[I_{GSabc}]$ is fixed, given by either (17) or (19), as it is explained in the next subsection.

C. Initial Powerflow Solution and Network Solution During Dynamic Simulation

To adequately initialize the dynamic simulation, the static powerflow solution of generator buses should consider the physical symmetry constraints of synchronous generators. The phase voltage and current unbalance of the generator buses cannot be freely determined due to their physical construction. The problem becomes more challenging for a microgrid set up where there is no strong substation bus. Therefore, no bus can be defined as having a known voltage magnitude and angle to serve as traditional slack bus. Note that a strong reference bus is assumed in both traditional transmission balanced powerflow and distribution unbalance powerflow, so this approach requires special considerations. This sub-section provides a method to arrive to a fully unbalanced solution, including the general case where no strong bus is present in the system. The network powerflow solution during dynamic simulation is also described. The key element of this solution is the assumption of generator physical symmetry constraints.

Generator physical symmetry constraints were first introduced in [16] for distributed generation modeled as PQ buses in a distribution network powerflow solution with presence of strong slack bus, where the voltage magnitudes and angles are known in advance. To accommodate islanded microgrid conditions, the symmetry constraint is extended to all generator buses. The traditional slack bus is used to obtain a first approximation of the solution. The slack bus constraint is relaxed in a second step to obtain the final solution, with unbalances at all buses for the general case. This process allows the overall powerflow solution to converge to an initial operating point, without using a fixed reference voltage traditional distribution powerflow solutions utilize.

To explain the solution process, define the following three types of buses:

- Type-1 bus is the traditional slack bus, where the voltage magnitudes and angles in each phase are given and are not updated as the powerflow algorithm iterates.
- Type-2 buses are generator PQ buses where their total power, $P_T = P_a + P_b + P_c$ and $Q_T = Q_a + Q_b + Q_c$, remain constant during iterations of the powerflow algorithm. Individual phase powers are allowed to change based on network unbalances and the generator symmetry constraints of (17) and (18). I_{GS1} and $[I_{GSa,b,c}]$ are also calculated from (17) and (18) and used in the powerflow solution as specified current in (21).

- Type-3 buses are generator buses with constant positive sequence-based current source values, $[I_{GSa,b,c}]$, behind the machine admittance matrix $[Y_{Ga,b,c}]$.

Note that in type-2 buses, the generator current source values are updated at each iteration of the powerflow solution to meet both the constant P_T and Q_T, as well as modeling the generator physical symmetry constraint (positive sequence current source behind $[Y_{Ga,b,c}]$). Additionally, type-3 buses are used for two purposes: 1) to link the machine dynamics with the network powerflow solution with (19), (13), and (14); and 2) to find the final initial powerflow solution with unbalances and symmetry constraints in all generator buses per the routine below.

The basic steps for the initial powerflow solution are:

1) Choose one generator bus as type-1 (traditional slack bus) and the rest of the generator buses as type-2 (generator PQ bus with symmetry constraint). Solve the initial powerflow using the method of [15] with the modifications described in Section III-A, while keeping track of P_T and Q_T at the type-1 bus.
2) Once initial convergence is reached, the current source value of the type-1 generator bus, $[I_{GSa,b,c}]$, is calculated using (17) and (18).
3) The type-1 bus is changed into a type-3 bus using its latest P_T and Q_T values to obtain the Norton equivalent current source value, I_{GS1}.
4) The powerflow is once again solved with all generator buses as type-3. That is with all generators represented as constant current sources behind machine admittances, reaching a final unbalanced solution for the initial powerflow subject to machine symmetry constraints.

Note that steps 2), 3), and 4) are not necessary for the case when the slack bus is a strong substation, in which case, step 1) is the final solution for the initial powerflow.

Once the initial powerflow solution is complete, the dynamic simulation is ready to start. The initial power flow solution is used to initialize the machine differential equations of Section II-A with the assumptions in Section III-A. All generator buses become type-3 buses and remain implemented as type-3 for the remainder of the dynamic simulation steps. The machine dynamic states, governed by the equations in Section II-A and assumptions in Section III-A, drive the system response by updating the Norton current sources through the link with the full network powerflow given in (19). In addition to capturing machine states behavior, the distribution-level powerflow can also capture explicit load state behaviors as in [4], completely recalculating the network solution at each dynamic simulation step.

These steps are essential to the effective dynamic modeling of distribution networks, including the case of isolated microgrids.

IV. Simulation and Validation

This section contains the simulation results for three different models, with computational times highlighted in a final sub-section. The first two models represent a validation of the proposed approach with an established, electromagnetic transients simulation software [2]. The third system represents a larger system and greater generator count, to insure the algorithm works for larger distribution microgrids. In all simulations, changes to the system are enacted to induce a significant response in the generators of the system. These larger responses are meant to demonstrate the behavior of the proposed approach under larger deviations from normal operations. Accurate models of microgrids and distribution systems of interest would likely include protective devices that would respond to such deviations, such as under-frequency and over-frequency relays. These items are omitted from these scenarios to focus on the proposed machine models and will be incorporated into future work and simulations.

TABLE I
Simple System Load Scenarios

Unbalance	Phase Power (kW,kvar)		
	A	B	C
0%	(1320,660)	(1320,660)	(1320,660)
10%	(1320,660)	(924,462)	(1716,858)
30%	(1320,660)	(528,264)	(2112,1056)

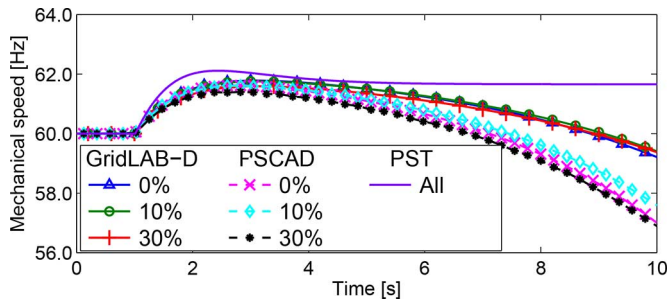

Fig. 1. Mechanical speed for simple system with three unbalance situations.

For this section, all implementations of the proposed approach were done and tested within the GridLAB-D software [18]. GridLAB-D is an open-source, agent-based simulation environment developed by the U.S. Department of Energy, Office of Electricity Delivery and Energy Reliability. Validation simulations were performed in Manitoba HVDC Research Centre's PSCAD software [2]. PSCAD is a full electromagnetic solver and GridLAB-D implements the proposed electromechanical method.

To obtain an additional insight on the results of the proposed model, the first validation test also contains a comparison with a standard positive-sequence dynamic simulator. The Power System Toolbox (PST) [21] serves as this simulator, which uses the standard type of model for transmission level analysis. This comparison serves as a point of reference with a more simplified model that is not suitable for distribution or microgrids, to give a sense of the accuracy of the proposed model.

A. Single Machine With Load Connected Through Unbalanced Distribution Line

A simple test system was used to evaluate the proposed synchronous machine modeling approach. The system consisted of a synchronous machine connected to a load through a non-transposed line. For the distribution line, the overhead line model with configuration 601 given in the IEEE 13-node test system data [22] was used, with a length of 1 mile. The three-phase load was a Wye-connected constant impedance load. Three load scenarios were created to achieve the different unbalances shown in Table I. The total three-phase power (3960 kW, 1980 kvar) is conserved in all load-step scenarios, only the unbalance is different. The disturbance used in each case consisted of a 10%-step reduction in load.

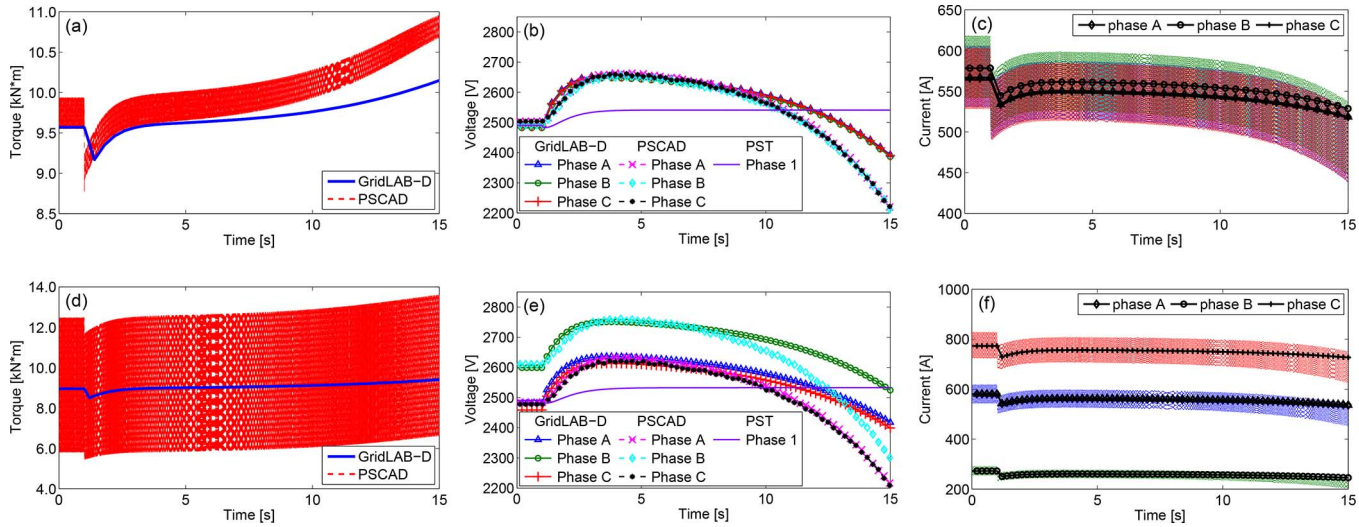

Fig. 2. Single machine simulation results of balanced system (a) electrical torque, (b) terminal voltage magnitude, and (c) terminal current magnitude and a 30% unbalanced system (d) electrical torque, (e) terminal voltage magnitude, and (f) terminal current magnitude.

This simulation represents a set of extremely basic cases to demonstrate a single machine's unbalanced operation, as well as validate the implemented generator control devices (governor and exciter) under the unbalanced conditions. A total of four cases were simulated. The first three cases considered the machine without a governor or exciter, with varying levels of unbalance in the load. The fourth case added machine controls for the 30% unbalance load case. The fourth case also replaces the step-change in load with a momentary single line-to-ground fault. The percent unbalance of each scenario was measured using the IEEE 1159 standard [23].

Fig. 1 shows the mechanical speed of the first three cases, representing different levels of unbalance in the load. Fig. 1 includes simulation results for the electromechanical method presented in this paper (labeled GridLAB-D), PSCAD electromagnetic simulations, as well as electromechanical simulations for the PST (positive-sequence only). Note that only one line is present for the PST case, since there is no method for properly representing the unbalanced load in the positive-sequence-only simulation; only the balanced case is presented.

Fig. 1 shows that the short-term transient response from GridLAB-D is nearly identical to the electromagnetic response from PSCAD. However after 5 seconds of simulation, the speed solutions begin to differ between GridLAB-D and PSCAD. This is a result of the electromechanical simplifications discussed in Sections II and III. Fig. 1 also shows the PST simulation having a similar transient behavior, but stabilizing to a different final point. The transient difference is a result of simplifications in the PST model similar to those mentioned in Sections II and III, as well as [6, ch. 5]. The PST does not easily include an electrical frequency-dependent method for varying impedance loads. Once the speed of the system begins to move off nominal, the GridLAB-D/PSCAD simulations are quickly representing a completely different system, resulting in the different final condition of the PST results.

Fig. 2(a) and (d) shows the electrical torques for the balanced and 30% unbalanced load step-change cases. The effect of the unbalance can be seen in the variation of the electrical torque in the PSCAD simulation. The torque variation observed in the balanced load case, Fig. 2(a), is due to the small unbalance introduced by the un-transposed distribution line. Fig. 2(d) demonstrates the electrical torque variation is larger due to the larger unbalance. In both cases, the proposed model approximates the moving average value of the electric torque of the validation simulations. The approximation of the proposed model in the first 5 s of the simulation is closer to PSCAD than in the portion between 5 to 15 s of simulation time. As the simulation progresses, the simplifications in the proposed model become more apparent, with the GridLAB-D and PSCAD results drifting apart.

The model comparison is completed with the terminal voltage and terminal current plots for the balanced and 30% unbalanced cases. The balanced and unbalanced scenario voltage magnitudes are shown in Fig. 2(b) and (e). PST results for the terminal voltage in the positive-sequence case are also included in both Fig. 2(b) and (e). The proposed electromechanical method (GridLAB-D) and PSCAD results match very well for the early part of the simulation and transient. Some minor differences are present in the initial values of the voltage, primarily due to the slight differences in the level of detail in the models. As the simulation progresses, the modeling differences between the GridLAB-D and PSCAD curves become more significant. This is associated with the simplifications and differences mentioned in Sections II and III, particularly those related to unmodeled speed-dependent terms.

Further shown in Fig. 2(b) and (e), the PST results differ significantly from both the proposed method and the PSCAD validation results. Similar to the speed difference noted earlier, most of these differences are attributed to simplifications and assumptions in models used in the PST simulation. These differences result in the system reaching its new operating point quicker than the GridLAB-D/PSCAD simulations, primarily due to the less detailed generator and load modeling. In particular, the positive-sequence representation contributes to some of the disparity, especially in the 30% unbalance case. The PST voltage only closely matches the initial Phase A and C voltages

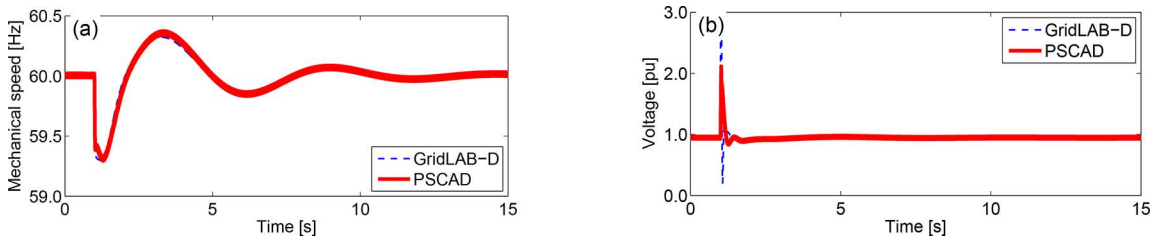

Fig. 3. Single-machine with control simulation results of (a) mechanical rotor speed and (b) field voltage.

for the 30% unbalanced case, but is significantly different than the Phase B value. On a much more complicated system, these differences could lead to significantly different loading on the system, further reinforcing the more accurate nature of the unbalanced GridLAB-D and PSCAD simulations.

Balanced and unbalanced scenario current magnitudes are shown in Fig. 2(c) and (f), respectively. Similar to the electrical torque values, the currents in the proposed model approximate the moving average value of the more detailed PSCAD model. The approximation is again more accurate in the first part of the simulation, but drifts away towards the end of the simulation. This is because the inherent differences between the proposed method and the PSCAD results become greater. These differences in currents are coupled with the differences observed in mechanical rotor speed of Fig. 1 and the voltages, resulting in a different "long-term" transient behavior between the electromagnetic and electromechanical models.

The simulations for the 30% unbalance load were ran again with two changes to the simulation. The first change is the addition of machine controls: a governor and AVR. As mentioned in Section II-D, a DEGOV1 governor and SEXS automatic voltage regulator (AVR) were utilized. The second adjustment changed the simulation from a load step change to a fault case. At 1.0 s into the simulation, a low impedance (1.0 ohm) line-to-ground fault is induced on phase A, half a mile from the generator bus (50% of the line length). This fault is cleared 24 milliseconds later, placing the system back in the original topological state.

Fig. 3(a) and (b) demonstrates that the responses of the machine mechanical speed and field voltage approximate the responses of the more detailed PSCAD simulation. Voltage and current magnitude results closely matched the PSCAD results and are omitted for brevity. Note that with controls on the machine model, the differences between the electromagnetic and electromechanical models are reduced. This is especially relevant when considering that nearly all operating synchronous machines will have some form of active controls. Uncontrolled synchronous generators are rarely deployed, so the fundamental differences between the two models do not impact practical simulations.

B. 13-Node, Two-Generator

The larger validation test for the proposed approach involved comparing simulation results from GridLAB-D and PSCAD using the IEEE 13-node distribution test feeder. Details of the feeder can be found in [22]. For this validation test, two identical 2.5-MVA generators with identical parameters, including governor and exciter, were attached to the 13-node system. These two generators were attached at the main three-phase backbone of the system, attached at node 650 and at node 671. No large transmission connection is assumed.

The modified IEEE 13-node system begins with the generators providing nearly 4.0 MVA of power. The generator response moving from this initial operating point was excited by tripping off a portion of the system. At 1.0 s in the simulation, the lateral associated with nodes 645 and 646 is switched out of the topology. This results in a loss of 400 kW and 257 kvar of load on phase B of the system, resulting in a final loading level of approximately 3.5 MVA. The loss of load on only a single phase of the system further influences the unbalanced conditions on the microgrid.

The loss of load will obviously influence the generators on the system. The most obvious influence is in the rotor speed of the generators. Fig. 4(a) shows the GridLAB-D and PSCAD responses in one of the generators to this sudden drop in load at 1.0 second. The two generators had nearly identical responses, which isn't unexpected given their identical parameters. As the figure demonstrates, the GridLAB-D and PSCAD results are nearly identical. Of special note here is the impact the time-varying torque values had on the results, shown in Fig. 4(b). Without the time-varying electrical and mechanical torque values, original results had GridLAB-D responding in a much faster fashion than PSCAD. Their inclusion highlights that while it is often possible to neglect such impacts on a larger system or in transmission-level studies, they have a significant influence in a smaller microgrid environment.

As with the simple machine examples in the previous subsection, the torque results demonstrate the largest difference in the extremely detailed PSCAD simulations and the reduced model implemented in GridLAB-D. With the unbalanced conditions on the system, the generator electrical torque varies significantly in the electromagnetic transient time range. As the figure demonstrates, GridLAB-D is tracking the moving average of this electrical torque, per the assumptions and simplifications stated in Section III. In spite of this obvious difference, the modeled "average" mechanical torque tracks a similar path as the explicit PSCAD model. Furthermore, the mechanical torque values are nearly identical and the rotor speeds are closely matched as well.

The largest impact this simplification has on the modeled results are on the terminal voltage magnitudes at the generator interconnect. Fig. 4(c) shows the terminal voltage magnitude at the substation-connected generator. As with the electrical torque, the more detailed electromagnetic PSCAD model produces a more varied voltage magnitude than the GridLAB-D produced model. However, as with the electrical torque, the moving average of the PSCAD-produced voltage magnitude

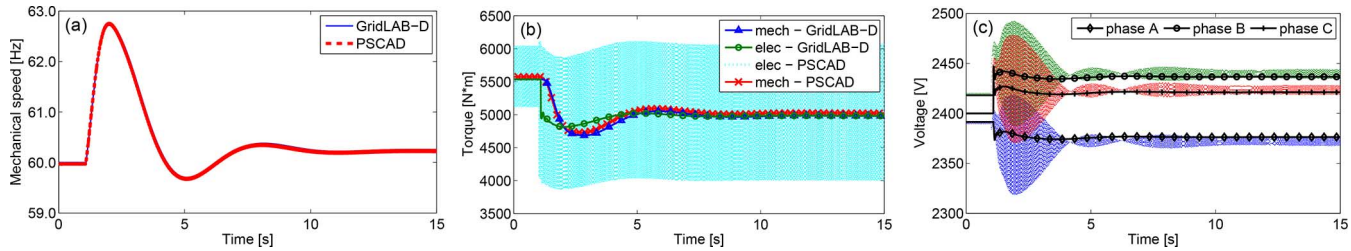

Fig. 4. IEEE 13-node simulation results of (a) mechanical rotor speed, (b) electrical and mechanical torque, and (c) terminal voltage magnitude.

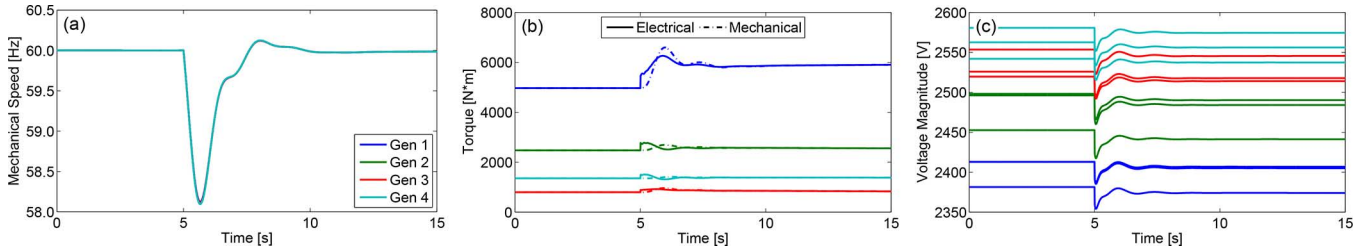

Fig. 5. IEEE 123-node simulation results of (a) mechanical rotor speed, (b) electrical and mechanical torque, and (c) terminal voltage magnitude. Specific colors represent the same generator in each subplot.

TABLE II
IEEE 123-NODE GENERATOR SIZE AND CONNECTIONS

Name	Size	Mode	Node
Gen 1	3.0 MVA	Isochronous	150
Gen 2	1.5 MVA	Droop	30
Gen 3	750 kVA	Droop	108
Gen 4	500 kVA	Droop	83

follows the same results as the GridLAB-D simulation. This matching represents the level of detail expected from the phasor-based simplifications of the model from Sections II and III.

C. 123-Node, Four-Generator

The final simulation case is built on the IEEE 123-node distribution test feeder [22]. This result was not validated against PSCAD because of the complexity of building large models in PSCAD, but it serves to show the proposed methods scale to larger systems. The system maintains the topology and initial loads of the standard IEEE 123-node feeder, but is no longer assumed to be connected to a larger transmission power source. Four distributed synchronous generators have been attached to various parts of the topology to provide power to the loads. Table II shows the generator sizes, governor operating mode, and connection points on the IEEE 123-node system. Each of these generators includes the governor and exciter models described earlier in the paper.

The simulation begins with the four generators providing roughly 3820 kVA of power to the system. At 5.0 s into the simulation, a simple, unbalanced step-load change occurred. This load change represented adding an additional 495 kVA of load onto the system. This represents a 427% increase in load at modification point and roughly 13% load increase on the overall feeder. The remainder of the simulation time demonstrates the four generators' control devices responding until a new power equilibrium is established. At this final operating point, the generators are providing approximately 4320 kVA of power.

Fig. 5(a) shows the mechanical rotor speed plot for all four generators on the system. The rotor speed initially drops to just above 58 Hz and then the governors on the generators begin responding to recover the frequency. Gen 1 operates as an isochronous generator for the system, driving the adjustment back to the 60-Hz nominal frequency value. Even with four generators interacting on a much larger system, the response is still able to demonstrate the significant frequency drop for this specific load change in a 19-s computation execution time. Such information is very useful for evaluating the required generator sizes, and controls, to prevent low frequency conditions during load starts. Simulating such an occurrence is the first step in evaluating how protective devices, such as under-frequency relays, would behave in an islanded feeder like the 123-node system simulated.

Fig. 5(b) shows the overlaid electrical and mechanical torque for each of the generators, still utilizing the same color designation as Fig. 5(a). Electrical torque for the generators is designated with a solid line and mechanical torque is a dashed line. After the initial increase in load, the governor responses begin adjusting the mechanical torque of the generators. The electrical torque on the system reflects and interacts with these changes as the system moves back toward the nominal rotor speed observed in Fig. 5(a). This reinforces the observation from the speed plot, indicating that the transient model still behaves properly with multiple generators interacting over a larger system.

The previous plots demonstrated that the governor controls continue to function well with a larger system and more generators, but the governors are only half of the control scheme on the generators; exciter controls must also be considered. Fig. 5(c) plots the voltage magnitudes of all three phases at each of the generator connection points, again keeping the same color designations. While the individual three-phase voltage magnitudes are plotted for each generator, individual phases are not distinguished. The overall imbalance of each generator is reflected by the three different voltage magnitude traces

TABLE III
MODEL EXECUTION TIMES FOR GRIDLAB-D AND PSCAD

Model	GridLAB-D Time (s)	PSCAD Time (s)
Balanced 2-node	8	81
10% unbalance 2-node	12	85
30% unbalance 2-node with control and step	12	79
30% unbalance 2-node with control and fault	18	81
IEEE 13-node	9	310
IEEE 123-node	22	N/A

associated with each generator. When the load decrease occurred, the exciter controls began adjusting the voltage back to determined band. The exciter controls only utilized the positive-sequence voltage, so effectively the average of the three phases must move back within the desired voltage band. This is the primary reason why the voltages do not adjust back to their pre-load-increase values.

The scaling to the larger system showed no unexpected interactions or problems with the new machine model, initialization routine, or the implemented governor or exciter models. While not validated against PSCAD, it does serve as an indication that scaling to a larger system will not immediately cause problems in the model. The model produced a level of detail appropriate for transient-level analysis of a microgrid with one or more synchronous machines present. With existing GridLAB-D distribution models, as well as the ability to convert topologies from other distribution formats, studies of different microgrid scenarios can quickly be explored using this model. Initial testing has confirmed that similar results are obtained with the IEEE 8500-node test system, further validating the scalability of the proposed work.

D. Computation Times for Different Models

Utilizing the proposed model to capture electromechanical behaviors, computation time for the different systems was reduced. The simulation times for the different models are shown in Table III. All simulations were conducted on a Core I7 3.40 GHz computer with 16 GB of RAM running Windows 7 Enterprise. GridLAB-D and PSCAD execution times are shown for the two-node and IEEE 13-node cases, while only the GridLAB-D time is shown for the 123-node case. Recall that a PSCAD validation of the 123-node system was not conducted due to the complexity of implementing such a larger system in the electromagnetic simulator's environment.

As Table III shows, GridLAB-D executes significantly faster than PSCAD for all simulations. On average, the electromechanical GridLAB-D model is 7 times faster than the PSCAD simulation of the same system. It is important to note once again that the primary reason for this shorter execution time is the simplification of the synchronous machine model to the approximate electromechanical dynamics, and the simplification of the network elements to algebraic quantities. Additionally, the simulation time step is 10 milliseconds in GridLAB-D, and 50 microseconds in PSCAD. PSCAD is clearly providing greater detail on the simulations. However, many system-level impact studies and evaluations of microgrids or distribution-systems do not require this level of detail, so the proposed, faster electromechanical simulations can be sufficient.

V. CONCLUSION

This paper has presented a method for the analysis of distribution- and microgrid-level dynamics on large-scale systems. This method is an extension of existing transmission-level practices to a more generalized three-phase, unbalanced representation. This has included the unbalanced modeling of synchronous machines, the end-use loads, and the integration of the two models into a single simulation framework. The presented method is an improvement over existing electromagnetic simulations because the simulations are significantly faster (7× or greater in this implementation), the system models can be directly imported from distribution planning models, and standard models for distribution equipment and end-use load models can be readily implemented. These improvements over existing techniques can facilitate faster, and more complete, analysis for capital projects where dynamics are an issue, especially for microgrids. While the presented work was performed in the GridLAB-D simulation environment, the formulation is extensible to any suitable simulation platform. Continuing work is focusing on how the presented method can be used as part of a standard planning process similar to how powerflow is used for steady-state analysis. It is expected that this process will inform the community on distribution and microgrid dynamics that have historically been addressed by installing equipment with larger than required ratings.

REFERENCES

[1] S. B. Van Broekhoven, N. Judson, S. V. T. Nguyen, and W. D. Ross, Microgrid Study: Energy Security for DoD Installations, Lincoln Lab., Lexington, MA, USA, Tech. Rep. 1164, Jun. 2012.
[2] Manitoba HVDC Research Centre, PSCAD Software, 2014 [Online]. Available: http://hvdc.ca/pscad
[3] A. Semlyen, J. F. Eggleston, and J. Arrillaga, "Admittance matrix model of a synchronous machine for harmonic analysis," *IEEE Trans. Power Syst.*, vol. 2, no. 4, pp. 833–839, Nov. 1987.
[4] K. P. Schneider, J. C. Fuller, and D. P. Chassin, "Multi-state load models for distribution system analysis," *IEEE Trans. Power Syst.*, vol. 26, no. 4, pp. 2425–2433, Nov. 2011.
[5] P. W. Sauer and M. A. Pai, *Power System Dynamics and Stability*. Champaign, IL, USA: Stipes, 2006.
[6] P. Kundur, *Power System Stability and Control*. New York, NY, USA: McGraw-Hill, 1994.
[7] P. Kundur and P. Dandeno, "Implementation of advanced generator models into power system stability programs," *IEEE Trans. Power App. Syst.*, vol. PAS-102, no. 7, pp. 2047–2054, Jul. 1983.
[8] B. Stott, "Power system dynamic response calculations," *Proc. IEEE*, vol. 67, no. 2, pp. 219–241, Feb. 1979.
[9] W. H. Kersting, *Dystribution Systems Modeling and Analysis*. Boca Raton, FL, USA: CRC, 2007.
[10] R. G. Harley, E. B. Makram, and E. G. Duran, "The effects of unbalanced networks on synchronous and asynchronous machine transient stability," *Electr. Power Syst. Res.*, vol. 13, no. 2, pp. 119–127, Aug. 1987.
[11] R. Salim and R. Ramos, "A model-based approach for small-signal stability assessment of unbalanced power systems," *IEEE Trans. Power Syst.*, vol. 27, no. 4, pp. 2006–2014, Nov. 2012.

[12] E. B. Makram, V. O. Zambrano, and R. G. Harley, "Synchronous generator stability due to multiple faults on unbalanced power systems," *Electr. Power Syst. Res.*, vol. 15, no. 1, pp. 31–39, Aug. 1988.
[13] E. Makram, V. Zambrano, R. Harley, and J. Balda, "Three-phase modeling for transient stability of large scale unbalanced distribution systems," *IEEE Trans. Power Syst.*, vol. 4, no. 2, pp. 487–493, May 1989.
[14] P. C. Krause, O. Wasynczuk, and S. D. Sudhoff, *Analysis of Electric Machinery and Drive Systems*. New York, NY, USA: Wiley, 2002.
[15] P. Garcia, J. Pereira, J. Carneiro, S. , V. da Costa, and N. Martins, "Threephase power flow calculations using the current injection method," *IEEE Trans. Power Syst.*, vol. 15, no. 2, pp. 508–514, May 2000.
[16] T.-H. Chen, M.-S. Chen, T. Inoue, P. Kotas, and E. Chebli, "Three-phase cogenerator and transformer models for distribution system analysis," *IEEE Trans. Power Del.*, vol. 6, no. 4, pp. 1671–1681, Oct. 1991.
[17] T.-H. Chen, M.-S. Chen, K.-J. Hwang, P. Kotas, and E. Chebli, "Distribution system power flow analysis—A rigid approach," *IEEE Trans. Power Del.*, vol. 6, no. 3, pp. 1146–1152, Jul. 1991.
[18] GridLAB-D Contributors, GridLAB-D Distribution Simulation Software, 2014 [Online]. Available: http://www.gridlabd.org
[19] GE Digital Energy, PSLF Software, 2014 [Online]. Available: http://gedigitalenergy.com/UOS.htm
[20] Siemens, PSS/E Software, 2014 [Online]. Available: http://www.energy.siemens.com/hq/en/services/power-transmission-distribution/power-technologies-international/software-solutions/pss-e.htm
[21] J. H. Chow, K. W. Cheung, and G. Rogers, Power Systems Toolbox, 2009 [Online]. Available: http://www.etk.ee.kth.se/personal/vanfretti/pst/Power_System_Toolbox_Webpage/PST.html
[22] IEEE PES Distribution System Analysis Subcommittee, Distribution Test Feeders, 2013 [Online]. Available: http://ewh.ieee.org/soc/pes/dsacom/testfeeders/index.html
[23] *IEEE Recommended Practice for Monitoring Electric Power Quality*, IEEE Std. 1159-2009 (Revision of IEEE Std. 1159-1995), Jun. 2009, pp. c1–81.

Marcelo A. Elizondo (S'98–M'07) received the Ph.D. degree in power system engineering from the Universidad Nacional de San Juan, Argentina, in 2008.

He joined Pacific Northwest National Laboratory (PNNL) in 2009. From 2003 to 2005, he was a graduate visiting scholar at Carnegie Mellon University, Pittsburgh, PA, USA, and he was an undergraduate visitor at Supelec, France, in 2001. He worked in Mercados Energéticos Consultores (Argentina) from 2007 to 2009, an international power system consulting firm. His research interests include power system dynamic modeling and control, microgrids, demand response, and HVDC systems.

Francis K. Tuffner (S'03–M'08) received the B.S., M.S., and Ph.D. degrees in electrical engineering from the University of Wyoming, Laramie, WY, USA, in 2002, 2004, and 2008, respectively.

He is currently with the Pacific Northwest National Laboratory as a power system engineer. His research interests include signal processing applied to power systems, PHEV integration, embedded control devices, distribution-level modeling, and digital signal processing.

Kevin P. Schneider (S'00–M'06–SM'08) received the B.S. degree in physics and the M.S. and Ph.D. degrees in electrical engineering from the University of Washington, Seattle, WA, USA.

His main areas of research are distribution system analysis and power system operations. He is currently a research engineer at the Pacific Northwest National Laboratory, working at the Battelle Seattle Research Center in Seattle. He is an Adjunct Faculty member at Washington State University and an Affiliate Assistant Professor at the University of Washington.

Dr. Schneider is a licensed Professional Engineer in Washington State. He currently serves as the Chair for the IEEE Distribution System Analysis Sub-Committee.